Comput Geosci (2014) 18:265–282
DOI 10.1007/s10596-014-9409-z

ORIGINAL PAPER

History matching of statistically anisotropic fields using the Karhunen-Loeve expansion-based global parameterization technique

Haibin Chang · Dongxiao Zhang

Received: 16 May 2013 / Accepted: 28 January 2014 / Published online: 1 March 2014

Abstract Traditional ensemble-based history matching method, such as the ensemble Kalman filter and iterative ensemble filters, usually update reservoir parameter fields using numerical grid-based parameterization. Although a parameter constraint term in the objective function for deriving these methods exists, it is difficult to preserve the geological continuity of the parameter field in the updating process of these methods; this is especially the case in the estimation of statistically anisotropic fields (such as a statistically anisotropic Gaussian field and facies field with elongated facies) with uncertainties about the anisotropy direction. In this work, we propose a Karhunen-Loeve expansion-based global parameterization technique that is combined with the ensemble-based history matching method for inverse modeling of statistically anisotropic fields. By using the Karhunen-Loeve expansion, a Gaussian random field can be parameterized by a group of independent Gaussian random variables. For a facies field, we combine the Karhunen-Loeve expansion and the level set technique to perform the parameterization; that is, for each facies, we use a Gaussian random field and a level set algorithm to parameterize it, and the Gaussian random field is further parameterized by the Karhunen-Loeve expansion. We treat the independent Gaussian random variables in the Karhunen-Loeve expansion as the model parameters. When the anisotropy direction of the statistically anisotropic field is uncertain, we also treat it as a model parameter for updating. After model parameterization, we use the ensemble randomized maximum likelihood filter to perform history matching. Because of the nature of the Karhunen-Loeve expansion, the geostatistical characteristics of the parameter field can be preserved in the updating process. Synthetic cases are set up to test the performance of the proposed method. Numerical results show that the proposed method is suitable for estimating statistically anisotropic fields.

Keywords Reservoir history matching · Statistically anisotropic field · Global parameterization · Karhunen-Loeve expansion

H. Chang (✉) · D. Zhang
ERE & LTCS, College of Engineering, Peking University, Beijing 100871, China
e-mail: haibinch@pku.edu.cn

1 Introduction

For reservoir development and management, a solid understanding of geological formation properties is extremely important for future production predictions and production optimization. Reservoir geological formation properties are always heterogeneous, and, due to limited knowledge, there are large uncertainties in the description of the formation properties. Sequential data assimilation of dynamic production data plays an important role in characterizing the formation properties and reducing uncertainty. A reliable history matching method can gradually update the uncertain model parameters to match the data and, at the same time, preserve the geostatistical characteristics of the model parameters. To achieve this aim, several methods have been developed, such as the gradual deformation method [3, 12, 14, 26] and the probability perturbation method [4, 5, 11, 13]. In its basic formulation, the gradual deformation algorithm uses a linear combination of two independent Gaussian random vectors with the same mean and covariance to produce a new Gaussian random vector that has the same geostatistical characteristics as the original

random vectors. In the data assimilation step, the deformation parameter is gradually updated to match the data [12, 26]. The gradual deformation method is also developed to perform an iterative calibration of sequential stochastic simulations [3, 14]. In addition to the gradual deformation method, the probability perturbation method is another method that can effectively preserve the geostatistical characteristics of the model parameters in the data assimilation process; it is achieved by perturbing the conditional probability model in the sequential simulation algorithm, rather than by directly updating the model parameters.

In recent years, ensemble-based history matching methods, such as the ensemble Kalman filter [1, 7, 23, 24] and iterative ensemble filters [10, 18, 30], have attracted a great deal of attention and have been successfully applied in the petroleum industry. The ensemble-based methods show superiority in their ease of implementation and their capability of dealing with large scale problems. The most common model parameters of the ensemble-based history matching method are spatially correlated rock properties, such as permeability and porosity. In the updating process of the history matching method, the parameter values at all the numerical grids are usually updated to match the observation data. The ensemble-based methods with grid-based model parameterization can be directly used for history matching of statistically anisotropic Gaussian field. For history matching of facies field with elongated facies, truncated plurigaussian is one of the popular approaches [2, 8, 17, 20]. The flexibility of grid-based model parameterization allows it to capture the local features of the unknown random field through data assimilation. Although there exists a parameter constraint term in the objective function for deriving ensemble-based methods [10, 18, 30] using a grid-based local parameterization, it is difficult to preserve the geological continuity of the parameter field in the updating process of these methods, especially in the estimation of statistically anisotropic field with uncertainties about the anisotropy direction. The geostatistical characteristics of a statistically anisotropic random field, such as anisotropy direction and directional correlation lengths, are difficult to characterize or preserve using a grid-based local parameterization technique.

Besides the grid-based local parameterization, there are some global parameterization techniques, including the Karhunen-Loeve (KL) expansion [9, 16, 21]. The KL expansion, which is a spectral expansion, transforms the correlated Gaussian random field into a group of independent variables. Because the variables in the KL expansion are independent, any realizations of these variables can provide a parameter field that honors the given correlation structure. The KL expansion is usually used as a parameterization or dimension reduction technique in the development of various methods. Reynolds et al. [25] discuss the use of the KL expansion for efficient parameterization. Zhang and Lu [32] develop a KL expansion-based moment equation (KLME) for uncertainty quantification of flow in porous media. In KLME, the parameter field is represented with the KL expansion, and the flow response quantities are decomposed by perturbation expansions. Sarma et al. [28] use the KL expansion to represent the parameter field and maintain the geological constraints in the development of a closed-loop reservoir production optimization method. Li and Zhang [19] use the KL expansion to parameterize the reservoir property fields and use polynomial chaos expansion to represent the flow response quantities in the development of the probabilistic collocation method for uncertainty quantification. Zhang et al. [33] use the KL expansion to parameterize the reservoir property fields and obtain the principle modes of the major source of the uncertainty in the development of the KL-based Kalman filter for data assimilation. Romary [27] uses the KL expansion of geostatistical models to reduce the dimension of the inference problem in the Monte Carlo Markov chains algorithm to increase its efficiency. There are some other global parameterization techniques, such as discrete cosine transform and polynomial chaos expansion. Jafarpour and McLaughlin [15] use discrete cosine transform to parameterize both model parameters and state variables, and the coefficients of the retained cosine basis function are updated with the data assimilation method. Zeng et al. [31] develop a probabilistic collocation-based Kalman filter (PCKF) for history matching. In PCKF, all the system parameters, states, and production data are approximated by the polynomial chaos expansion.

In this work, we propose a KL expansion-based global parameterization technique that is combined with the ensemble-based history matching method for inverse modeling of statistically anisotropic fields. For a spatially distributed Gaussian field, the geostatistical characteristics are the mean, variance, and covariance model. To preserve the geostatistical characteristics of a Gaussian field in the history matching process, the KL expansion is a proper parameterization technique. For a Gaussian random field with a known mean, variance, and covariance model, by using the KL expansion, it can be parameterized by a group of independent Gaussian random variables. For a facies field, we combine the KL expansion and the level set technique to perform the parameterization; that is, for each facies, we use a Gaussian random field and a level set algorithm to parameterize it, and the Gaussian random field is further parameterized by the KL expansion. The global model parameters of the Gaussian field or facies field are the independent Gaussian random variables. When the anisotropy direction of the statistically anisotropic field is uncertain, we also treat it as a model parameter. We adopt an iterative ensemble filter, the ensemble randomized

maximum likelihood filter, to perform the history matching. The performance of the proposed method is tested by synthetic cases.

This paper is organized as follows: We introduce the KL expansion-based parameterization and the ensemble randomized maximum likelihood filter in Sections 2 and 3, respectively. The case studies are given in Section 4. Some conclusions and discussions are presented in Section 5.

2 KL expansion-based parameterization

2.1 Karhunen-Loeve expansion

Let $Y(\mathbf{x}, \omega)$ be a random field, where $\mathbf{x} \in D$ (the physical domain) and $\omega \in \Omega$ (the probability space). One may write $Y(\mathbf{x}, \omega) = \bar{Y}(\mathbf{x}) + Y'(\mathbf{x}, \omega)$, where $\bar{Y}(\mathbf{x})$ is the mean and $Y'(\mathbf{x}, \omega)$ is the fluctuation. The correlation structure of the random field may be described by the covariance $C_Y(\mathbf{x}, \mathbf{y}) = \langle Y'(\mathbf{x}, \omega) Y'(\mathbf{y}, \omega) \rangle$. Since the covariance is bounded, symmetric, and positive-defined, it may be decomposed as follows [9]:

$$C_Y(\mathbf{x}, \mathbf{y}) = \sum_{n=1}^{\infty} \lambda_n f_n(\mathbf{x}) f_n(\mathbf{y}), \tag{1}$$

where λ_n and $f_n(\boldsymbol{x})$ are eigenvalues and eigenfunctions, respectively, and can be solved from the following Fredholm equation:

$$\int_D C_Y(\boldsymbol{x}, \boldsymbol{y}) f(\boldsymbol{x}) d\boldsymbol{x} = \lambda f(\boldsymbol{y}). \tag{2}$$

Then the random field $Y(\mathbf{x}, \omega)$ can be expressed as follows:

$$Y(\mathbf{x}, \omega) = \bar{Y}(\mathbf{x}) + \sum_{n=1}^{\infty} \sqrt{\lambda_n} f_n(\mathbf{x}) \xi_n(\omega), \tag{3}$$

where $\boldsymbol{\xi}_n(\omega)$ are independent Gaussian random variables with a 0 mean and unit variance when Y is assumed to be Gaussian. The expansion in Eq. 3 is called the Karhunen-Loeve (KL) expansion. The KL expansion, which is a spectral expansion, is optimal with a mean square convergence when the underlying process is Gaussian [9]. As such, one may truncate the infinite series of Eq. 3 with a finite number (N) of terms. From Eq. 3, one can get $\mathrm{Vol}(D)\sigma_Y^2 = \sum_{n=1}^{\infty} \lambda_n$, where $\mathrm{Vol}(D)$ is the domain size and σ_Y^2 is the variance of $Y(x, \omega)$. The decay rate of λ_n determines the number of terms that are retained in the KL expansion, which determines the retained random dimensionality (N) and the retained percentage of energy $\left(\sum_{n=1}^{N} \lambda_n / \sum_{n=1}^{\infty} \lambda_n \right)$ of the problem.

Although, in general, the eigenvalue problem in Eq. 2 has to be solved numerically, analytical or semi-analytical solutions exist under certain conditions. For a one-dimensional random field with an exponential covariance function $C_Y(x_1, y_1) = \sigma_Y^2 \exp(-|x_1 - y_1|/\eta)$, where σ_Y^2 and η are the variance and the correlation length of the random field, respectively, the eigenvalues and their eigenfunctions can be expressed as follows [32]:

$$\lambda_n = \frac{2\eta\sigma_Y^2}{\eta^2 w_n^2 + 1}, \tag{4}$$

and

$$f_n(x) = \frac{1}{\sqrt{(\eta^2 w_n^2 + 1)L/2 + \eta}} \times \Big[\eta w_n \cos(w_n x) + \sin(w_n x) \Big], \tag{5}$$

where w_n are positive roots of the characteristic equation:

$$(\eta^2 w^2 - 1) \sin(wL) = 2\eta w \cos(wL). \tag{6}$$

Equation 6 has an infinite number of positive roots. If the roots w_n are sorted in an increasing order, the related eigenvalues λ_n decrease monotonically.

For problems in multidimensions, if we assume that the covariance function is a separable exponential function, $C_Y(\boldsymbol{x}, \boldsymbol{y}) = \sigma_Y^2 \exp(-|x_1 - y_1|/\eta_1 - |x_2 - y_2|/\eta_2)$ for a rectangular domain $D = \{(x_1, x_2) : 0 \le x_1 \le L_1, 0 \le x_2 \le L_2\}$, the eigenvalues and eigenfunctions can be obtained by combining those in each dimension. For the statistically anisotropic fields, we select the major and minor correlation directions as the two coordinates of the covariance model. The coordinate system of the covariance model may be different from the reservoir coordinate system. How to generate the statistically anisotropic fields using KL expansion is discussed in Section 4.

2.2 Global parameterization

In reality, there exist some statistically anisotropic reservoir parameter fields. Figure 1a shows a statistically anisotropic Gaussian field, which has a large correlation length difference between the major and minor correlation directions. Figure 1b, c shows the facies field with elongated facies. The most common parameterization technique for these fields is the grid-based local parameterization. For example, a Gaussian random field, $Y(\mathbf{x}, \omega)$, can be parameterized by the property values at all or some of the grid blocks, $Y(\mathbf{x}_i, \omega), i = 1, ..., m$, where m is the number of the grid blocks used for parameterization. Each of these parameters is related to a physical location and will determine the property at its location or a local region near its location.

Using a numerical grid-based local parameterization technique is difficult to preserve the geostatistical characteristics of the parameter field in the history matching process,

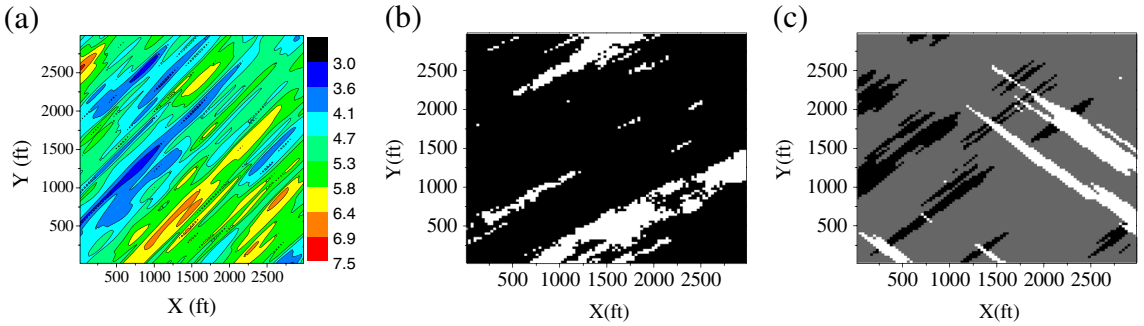

Fig. 1 Statistically anisotropic random fields. **a** Gaussian field. **b** Facies field with one elongated facies (the *white shade*). **c** Facies field with two elongated facies (the *white shade* and the *black shade*)

and illustrative examples will be given in Section 4. To preserve the geostatistical characteristics of the parameter field during history matching, the KL expansion is a proper global parameterization technique. In the following, we will discuss how to parameterize a Gaussian field and a facies field using the KL expansion, respectively.

2.2.1 Parameterization of a statistically anisotropic Gaussian field

For a second-order stationary Gaussian random field with a known mean, variance, and covariance model, by using the KL expansion, the model parameters, $\boldsymbol{m}$, are the same independent Gaussian random variables as those in Eq. 3. Then we have

$$\boldsymbol{m} = [\xi_1, \xi_2, ..., \xi_N]^T. \tag{7}$$

These variables have global properties, that is, they are not related to physical locations, and each of these variables will affect the parameter field distribution in the whole physical domain. Because these variables are independent, any realizations of these variables can provide a parameter field that honors the given covariance model.

For the kind of parameter field shown in Fig. 1a, the anisotropy direction (the major correlation direction), θ, is an important factor and may be associated with uncertainty. If θ is uncertain, we treat it as a model parameter. Under this condition, the model parameter for the Gaussian random field takes the following form:

$$\boldsymbol{m} = [\theta, \xi_1, \xi_2, ..., \xi_N]^T. \tag{8}$$

2.2.2 Parameterization of a facies field with elongated facies

To parameterize the facies fields as shown in Fig. 1b, c, we introduce the level set idea to perform the parameterization [6]. For a reservoir with one facies, the parameter field $p(\boldsymbol{x})$ can be written as follows:

$$p(\mathbf{x}) = p_f H(\Phi(\mathbf{x})) + p_n(1 - H(\Phi(\mathbf{x}))) \tag{9}$$

where $\Phi(\mathbf{x})$ is the level set function, H is the Heaviside function, and the coefficients p_f and p_n are the parameter values for the facies and normal reservoir medium, respectively. Furthermore, we define $\Phi(\mathbf{x}) = Y(\mathbf{x}) - a$, where $Y(\mathbf{x})$ is the second-order stationary Gaussian field for indicating the occurrence of facies; a is a predefined constant. When there are multi-facies types in the reservoir, we first parameterize each facies distribution independently. For facies i, we define $\Phi_i(\mathbf{x}) = Y_i(\mathbf{x}) - a_i$, and the distribution of facies i is determined by using Eq. 9 with $p_f = p_{f_i}$. Then the reservoir parameter field is composed by combining all the facies distributions. For the location passed by multiple facies, we need to determine a facies type that occupies the location. This should be done according to the understanding of the formation sequence of all the facies from the prior geological knowledge. If the prior geological knowledge is not enough to determine the formation sequence of the facies and the intersection area of different facies is large, a parameterization of the formation sequence should be taken. The geostatistical properties of $Y_i(\mathbf{x})$ should be designed according to the characteristics of facies i. The value of a_i should be designed according to the proportion of facies i. We denote the mean and the standard deviation of $Y_i(\mathbf{x})$ as μ and σ, respectively. Considering the definition of the level set function, if the proportion of facies i is prop_i, then a_i should satisfy

$$\frac{1}{\sqrt{2\pi}\sigma}\int_{a_i}^{+\infty} e^{-\frac{(t-\mu)^2}{2\sigma^2}}\,\mathrm{d}t = \text{prop}_i. \tag{10}$$

In order to preserve the geostatistical characteristics of each facies in the updating process, we use the KL expansion to parameterize the Gaussian field that is used for indicating each facies. For a facies field with n_f facies types, if we assume that the proportion and geostatistical characteristics

of each facies are known, then the model parameter takes the following form:

$$\boldsymbol{m} = \Big[\xi_{1,1}, \xi_{1,2}, ..., \xi_{1,N_1}, \xi_{2,1}, \xi_{2,2}, ..., \xi_{2,N_2}..., \xi_{n_f,1}, \xi_{n_f,2}, ..., \xi_{n_f,N_{n_f}}\Big]^T, \quad (11)$$

where $N_1, N_2, ..., N_{n_f}$ denote the number of retained terms in the KL expansion of each Gaussian random field. If the anisotropy direction of each facies is uncertain, the model parameter takes the following form:

$$\boldsymbol{m} = \Big[\theta_1, \theta_2, ..., \theta_{n_f}, \xi_{1,1}, \xi_{1,2}, ..., \xi_{1,N_1}, \xi_{2,1}, \xi_{2,2}, ..., \xi_{2,N_2}..., \xi_{n_f,1}, \xi_{n_f,2}, ..., \xi_{n_f,N_{n_f}}\Big]^T, \quad (12)$$

where $\theta_1, \theta_2, ..., \theta_{n_f}$ denote the anisotropy direction of each facies.

From the above, we can see that combining the KL expansion and the level set algorithm can parameterize a facies field by a group of global model parameters. An important step of the parameterization process is to design the geostatistical properties of the Gaussian field according to the characteristics of each facies. For a second-order stationary Gaussian random field, the geostatistical properties contain the mean, variance, covariance model type, correlation direction, and directional correlation lengths. The mean value can be set to any constant because it only impacts the value of parameter a. For the facies cases in this paper, we set the mean to be 0. The variance should not be too large because, otherwise, the uncertainty of the generated Gaussian fields will be large, which will increase the difficulty of the ensemble convergence. Also, if the variance is too small, the generated Gaussian fields will be too sensitive to the innovation. For the facies cases in this paper, we set the variance to be 0.5. The covariance model type can be set to common type, such as the Gaussian type or exponential type. For the facies cases in this paper, we choose exponential covariance model because of its analytical solutions of the eigenvalue problem. The major correlation direction of the Gaussian field should be the same as the facies elongated direction. The directional correlation lengths should be designed according to the directional facies mean length, which could be achieved through prior test. For a two-dimensional problem, let $l_i^{\text{prior}}, i = 1, 2$, denoting the facies mean length in the major and minor correlation directions obtained by prior geological information. We first set the initial guess of correlation lengths of the Gaussian field as $\eta_i^0 = \alpha l_i^{\text{prior}}, i = 1, 2$, where α is a coefficient. With this initial choice of η, we generate M set of Gaussian random fields and obtain the facies distributions using Eq. 9. The facies mean length of each generated realization is calculated by statistics and denoted by $l_i^1\left(\eta^0\right), ..., l_i^M\left(\eta^0\right), i = 1, 2$. Let $l_i^{\text{mean}} = \frac{1}{M}\sum_{n=1}^{M} l_i^n\left(\eta^0\right), i = 1, 2$. By comparing l_i^{prior} and l_i^{mean}, if η^0 is not the value we need, we decrease (or increase) η_i^0 by $\Delta\eta_i$ step by step until we get the region that contains the solution as $\left[\eta_i^0 - (n+1)\Delta\eta_i, \eta_i^0 - n\Delta\eta_i\right]$ $\left(\text{or}\left[\eta_i^0 + n\Delta\eta_i, \eta_i^0 + (n+1)\Delta\eta_i\right]\right)$. In the following, we can only check the midpoint of the region to get a new solution region, which is half of the previous region. Considering that $l_i^{\text{mean}}(\eta)$ is a monotonic function, with this procedure, we can refine the solution we wanted. The recommended values for α and $\Delta\eta_i$ are 1 and $0.5l_i^{\text{prior}}$, respectively.

3 Ensemble randomized maximum likelihood filter

Using the global model parameterization technique for history matching, there will be large modification to the parameter fields after the data assimilation, especially when the model parameters contain the anisotropy direction of the random field, which will increase the inconsistency problem of the history matching method that updates the model parameters and state variables simultaneously [29], such as the ensemble Kalman filter. To obviate the inconsistency problem and enhance convergence, in this work, we choose an iterative ensemble filter, the ensemble randomized maximum likelihood filter (EnRML), for history matching. Here, we briefly introduce the algorithm of EnRML, additional details of which are given by Gu and Oliver [10]. In EnRML, the model parameter update algorithm is

$$\begin{aligned}\boldsymbol{m}_j^{l+1} = {} & \beta_j^l m_{\text{pr},j} + \left(1 - \beta_j^l\right)\boldsymbol{m}_j^l \\ & -\beta_j^l C_{\text{M}} G_l^T \left(C_{\text{D}} + G_l C_{\text{M}} G_l^T\right)^{-1} \\ & \times \left[g\left(\boldsymbol{m}_j^l\right) - \boldsymbol{d}_{\text{obs},j} - G_l\left(\boldsymbol{m}_j^l - \boldsymbol{m}_{\text{pr},j}\right)\right] \\ & j = 1, ..., N_e,\end{aligned} \quad (13)$$

where l denotes the iteration index, j denotes the realization index, β denotes the step length factor, m_{pr} denotes the prior estimation of $\boldsymbol{m}$, C_{M} denotes the model parameter covariance, C_{D} denotes the observation error covariance, G_l denotes the ensemble average sensitivity matrix, $g(m)$ denotes model prediction observation, d_{obs} denotes the observation data, and N_e denotes the number of realizations.

At every data observation step, the updating process will be performed. Let M_{pr} be the matrix whose columns consist of model parameter vectors after the assimilation of all previous data. The model parameter covariance, which is prior to the assimilation of the current data but after the assimilation of all previous data, can be calculated by

$C_{\mathrm{M}} = \Delta M_{\mathrm{pr}} \Delta M_{\mathrm{pr}}^T / (N_e - 1)$, where ΔM_{pr} denotes the matrix of deviations from the means of the prior variables. The ensemble average sensitivity matrix changes with each iteration. At the lth iteration, let ΔD^l represent the deviation of each vector of computed data from the mean vector of computed data, and let ΔM^l represent the deviation of each vector of model variables from the current mean. The ensemble average sensitivity matrix can be calculated by

$$\Delta D^l = G_l \Delta M^l \tag{14}$$

where ΔM^l is $N_{\mathrm{M}} \times N_e$, ΔD^l is $N_{\mathrm{D}} \times N_e$, and G_l is $N_{\mathrm{D}} \times N_{\mathrm{M}}$. N_{M} is the number of model parameters, and N_{D} is the number of data. The model prediction observation is obtained by running the reservoir simulation from time 0 to the current observation step.

To evaluate the quality of the updated model parameters, a data mismatch function is defined as follows:

$$S(M) = \sum_{j=1}^{N_e} \left(g(\boldsymbol{m}_j) - \boldsymbol{d}_{\mathrm{obs},j}\right)^T C_D^{-1} \left(g(\boldsymbol{m}_j) - \boldsymbol{d}_{\mathrm{obs},j}\right) \tag{15}$$

The convergence criteria are defined as follows:

1. $\mathrm{MAX}_{1 \le i \le N_M; 1 \le j \le N_e} \left| m_{i,j}^{l+1} - m_{i,j}^{l} \right| < \varepsilon_1$,
2. $S\left(M^{l+1}\right) - S\left(M^{l}\right) < \varepsilon_2 S\left(M^{l}\right)$,
3. Iteration exceeds the preset maximum number of iterations, I_{MAX}.

4 Case studies

In this section, the proposed global parameterization technique is used in the EnRML process to estimate the statistically anisotropic fields. A synthetic two-dimensional reservoir model is set up. The reservoir is a square with a side length of 3,000 ft, and is evenly divided into 100 grid blocks in both directions. The reservoir has a thickness of 60 ft and is located at a depth of 4,000 ft. There are nine producers and four injectors in the reservoir, and the well locations are shown in Fig. 2. The producers are controlled by the bottom-hole pressure (BHP) constraint of 1,000 psi. The injectors are controlled by the surface flow rate target of 2,000 stb/day and are subjected to the maximum BHP constraint of 6,000 psi. The injection starts on the first day of production. The observations are obtained from running the reservoir simulation with a given reference parameter field. The observation data include the oil production rate, the water cut of the producers, and the bottom-hole pressure of the injectors. The simulation for acquiring observation data lasts for 510 days. The observations are available at the interval of 30 days, and then there are 17 observation steps. In the following subsections, three kinds of parameter fields are selected as the reference parameter fields. The performance of the proposed method is discussed.

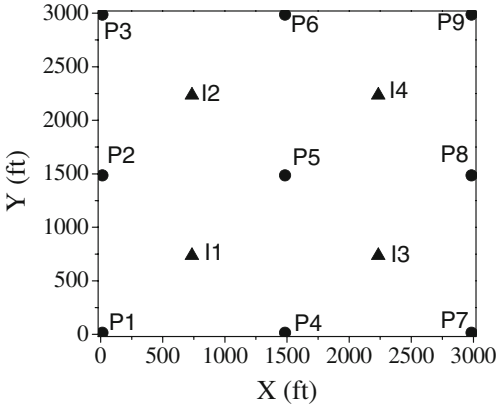

Fig. 2 The well locations

4.1 Case 1: statistically anisotropic Gaussian field

In this subsection, we discuss the history matching of a statistically anisotropic Gaussian field. The permeability field is the unknown random field that satisfies lognormal distribution. We assume that the geostatistical properties of ln k are known. The mean and variance are 5.0 + ln mD and 0.5, respectively. The covariance follows the separable exponential model. The major correlation direction is 45° with the positive x direction. The correlation lengths in the major and minor correlation directions are 1,500 and 150 ft, respectively. Figure 1a shows one example of the ln k field, which is selected as the reference field. The corresponding observation data for the history matching method are generated through reservoir simulation. The measurement errors are drawn from a 0-mean Gaussian distribution, and the standard deviation is set to 3 % of the actual measurement. The statistical property of the measurement errors is the same for all of the following cases.

We use the KL expansion to parameterize the described Gaussian random field to obtain the global model parameters. The number of retained terms in the KL expansion in the major and minor correlation directions is 8 and 80, respectively; thus, there are a total of 640 independent Gaussian random variables, which are the global model parameters. The retained energy is about 90 % of the total energy, which is assumed to be sufficient for the approximation. For EnRML, we set $\varepsilon_1 = 10^{-4}$, $\varepsilon_2 = 10^{-3}$, $I_{\mathrm{MAX}} = 2$, and $N_e = 100$. The error tolerance (ε_1 and ε_2) and the number of realizations (N_e) are the same for all of the following cases, but the preset maximum number of iterations (I_{MAX}) is different for different cases. The initial realizations of the ln k field are generated by

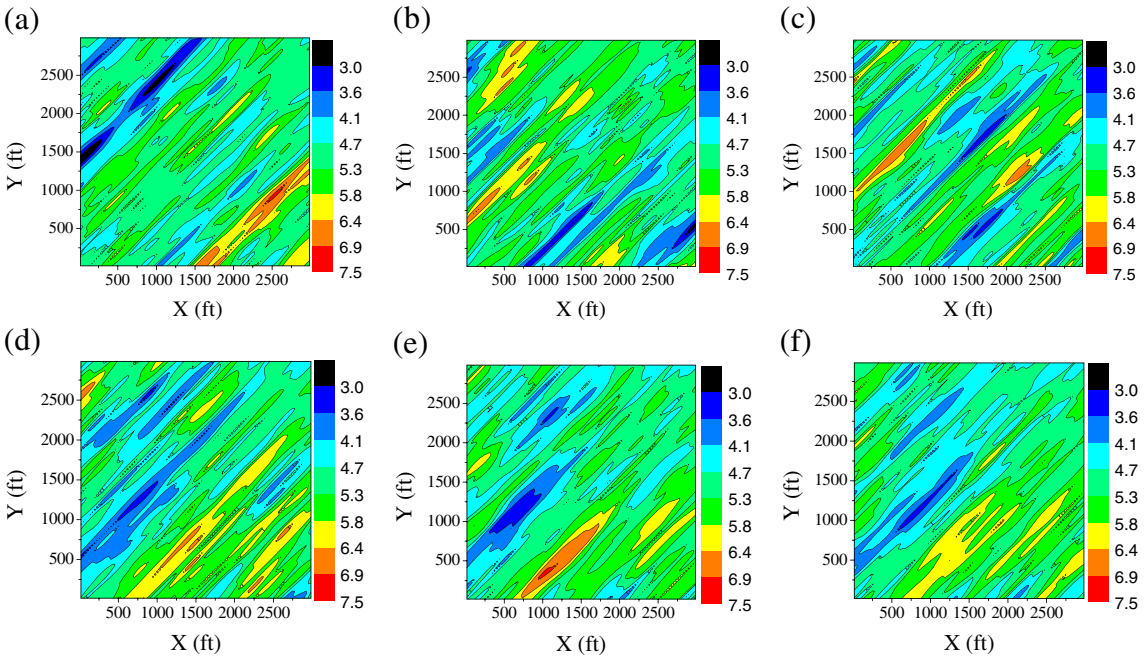

Fig. 3 Three initial realizations of the Gaussian random field (**a–c**) and the corresponding updated realizations (**d–f**)

sampling the independent Gaussian random variables (that have a 0 mean and unit variance) in the KL expansion. Figure 3a–c shows three initial realizations of the ln k field. From these figures, we can see that the generated initial realizations have the same geostatistical characteristics as the reference; however, the spatial distributions differ from each other and from the reference. We then perform the EnRML algorithm to update those global model parameters, and the updated global model parameters are used to construct the new ln k field. Figure 3d–f shows three updated realizations of the ln k field. By comparing these figures with Fig. 1a, we can see that the updated realizations can capture the features of the reference field well, and the geostatistical characteristics of the random field are preserved in the updating process. Figure 4 shows the match of the oil production rates and the forecast of three producers from the initial ensemble (Fig. 4a–c) and the updated ensemble (Fig. 4d–f). The simulations run from time 0 to day 900 with

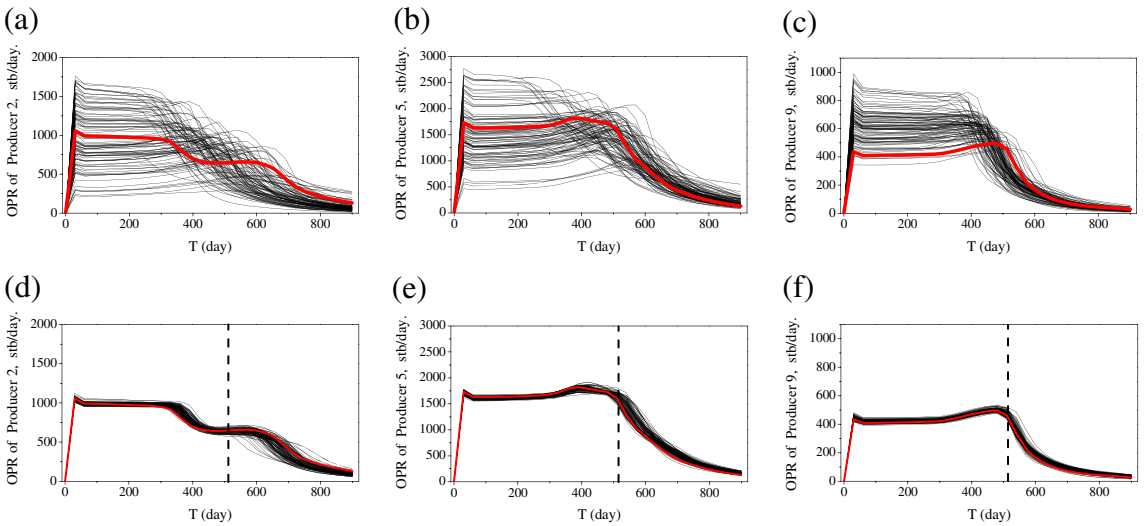

Fig. 4 The match to the oil production rates and the forecast of three producers from the initial ensemble (**a–c**) and the updated ensemble (**d–f**). In these figures, the *red line* indicates the oil production rate from the reference, the *black lines* indicate the oil production rates from the ensemble, and the *vertical dash lines* indicate the beginning of forecast

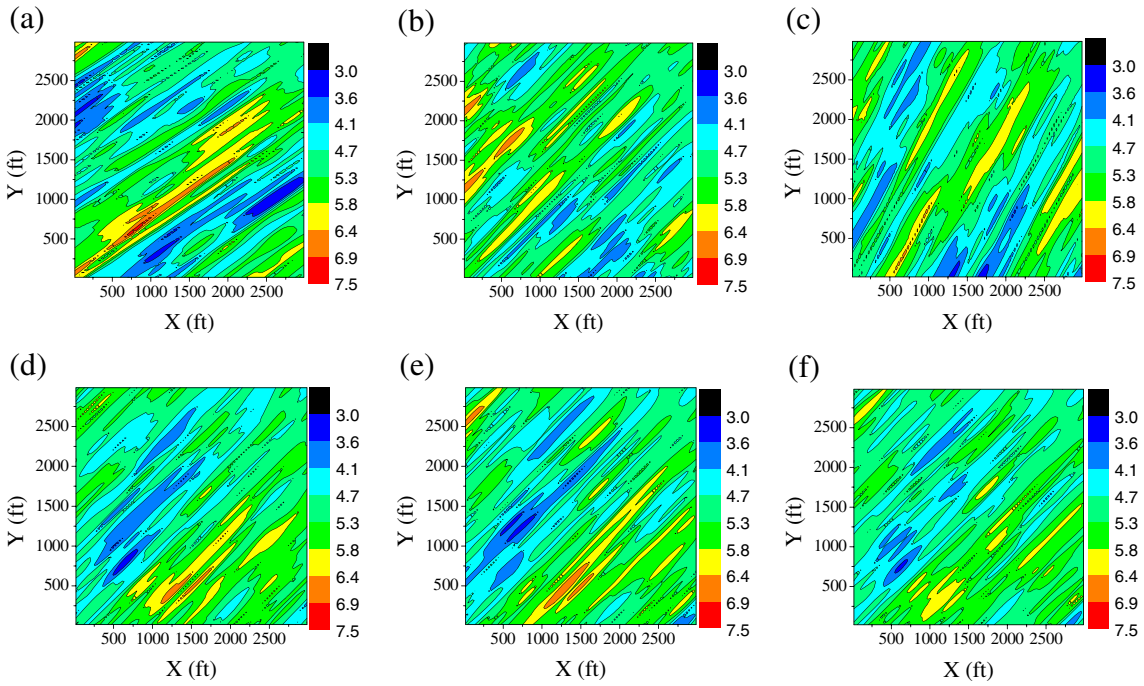

Fig. 5 Three initial realizations of the Gaussian random field with uncertain anisotropy direction (**a**–**c**) and the corresponding updated realizations (**d**–**f**)

the initial ensemble and the updated ensemble as parameter input, respectively. Thus, the results in the last 390 days are pure forecasts. In Fig. 4d–f, the vertical dash lines indicate the beginning of forecast. From these figures, we can see that, after data assimilation, the uncertainties in the initial ensemble are greatly reduced, and the production behavior from the updated ensemble can match the reference well and can provide reliable forecast. From this case, we can see that the KL expansion-based global parameterization technique can be properly used in the history matching method to estimate the statistically anisotropic Gaussian random field and to preserve the geostatistical characteristics of the random field in the updating process. In this case, we do not use the parameter value measurements at the well locations; if this kind of data is available, a conditional KL expansion can be used to perform the proposed algorithm [22].

For a statistically anisotropic Gaussian random field, the anisotropy direction (also the major correlation direction), θ, is an important factor and may be associated with uncertainty. Here, we further investigate the history matching problem described above with the assumption that θ is uncertain. At this time, the model parameter takes the same form as that in Eq. 8. In addition to the independent Gaussian random variables, the model parameters contain the anisotropy direction. For the reference field, θ equals 45 (the degree with the positive x direction), and this is the reference value. For the initial ensemble, we suppose that θ follows the uniform distribution of $U[25, 65]$. The

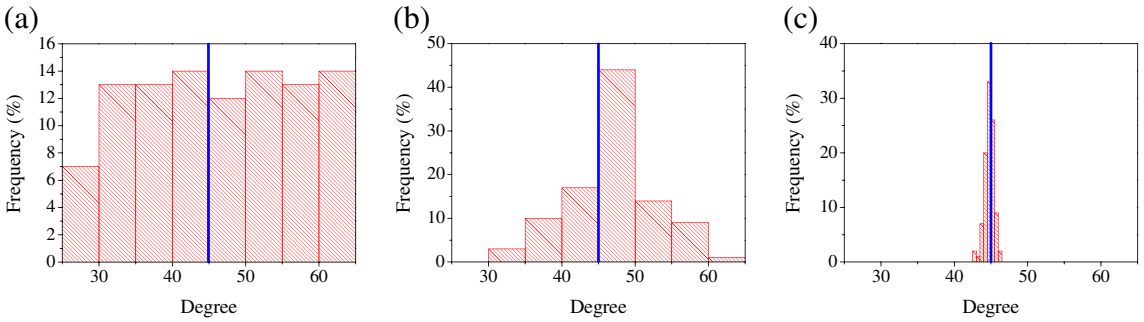

Fig. 6 Histogram of the anisotropy direction from the initial ensemble (**a**), the updated ensemble at step 3 (**b**), and the updated ensemble at step 10 (**c**). The *blue vertical line* indicates the reference value

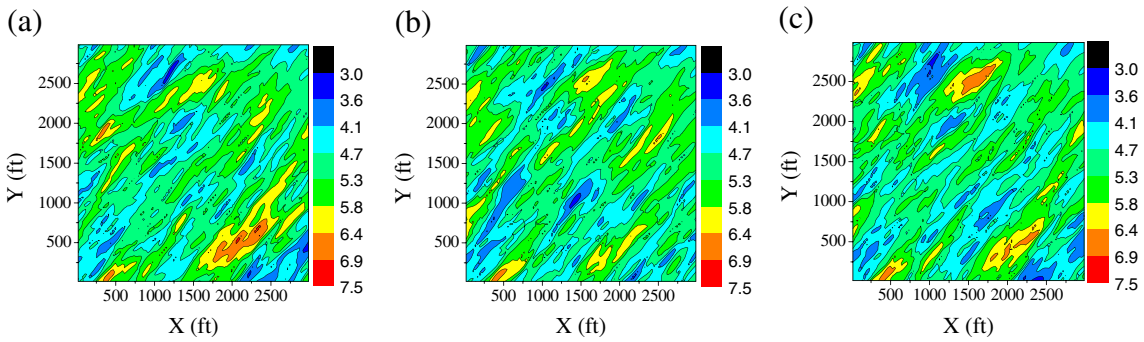

Fig. 7 Three updated realizations of the Gaussian random field with uncertain anisotropy direction using the grid-based parameterization in the history matching method

initial realizations of the ln k field are generated by sampling of $\{\xi_i\}_{i=1}^{N}$ in the KL expansion and θ. We select the major and minor correlation directions as the two coordinates of the separable exponential covariance model. To simplify the problem, we assume that the directional correlation lengths are not varying. Then, the eigenvalue and eigenfunction have to be solved only once. For each realization of $\{\xi_i\}_{i=1}^{N}$, we generate a random field realization in the coordinate system of the covariance model. Furthermore, we perform a coordinate rotation, with respect to the realization of θ, to obtain the random field realization in the reservoir coordinate system. Figure 5a–c shows three initial realizations of the ln k field. From these figures, we can see that the generated initial realizations have different anisotropy directions and that the spatial distributions are different from the reference. We then perform the EnRML algorithm to update those global model parameters. Here, we increase the preset maximum number of iterations to four, i.e., $I_{\mathrm{MAX}} = 4$. Figure 5d–f shows three updated realizations of the ln k field. By comparing these figures with Fig. 1a, we can see that the updated realizations can capture the features of the reference field well. Figure 6 shows the histogram of the anisotropy direction from the initial ensemble and the updated ensemble at step 3 and step 10. We can see that the updated ensemble at step 3 shows a tendency to converge to the reference value and that the updated ensemble at step 10 has a good convergence. From this case, we can see that, when the anisotropy direction of the random field is uncertain, it can be treated as a model parameter and an accurate estimation can be obtained using the proposed method.

In order to test the necessity of the KL expansion-based parameterization technique used for estimating the statistically anisotropic field with uncertain anisotropy direction and preserving the geostatistical characteristics, we add one more case. In this case, the initial realizations shown in Fig. 5a–c are updated using a grid-based parameterization, i.e., the ln k values at all the numerical grids are the model parameters and are updated at the data assimilation steps. Figure 7 shows three updated realizations, from which we can see that the updated realizations cannot capture the features of the reference well. Furthermore, the geostatistical characteristics, such as the large correlation length in the major correlation direction, are not preserved for each realization. The updated results show a tendency to capture the reference anisotropy direction, but cannot provide an accurate estimation. In deriving the ensemble-based method, there exists a constraint term in the objective function, which constrains the deviation of the updated model parameter from the prior estimation. However, there does not exist a constraint term that constrains the model parameter to preserve the geostatistical characteristics. So, it is not appropriate to use a grid-based parameterization technique for the history matching of statistically anisotropic field with uncertain anisotropy direction.

4.2 Case 2: facies field with one elongated facies

In this subsection, we discuss the history matching of a facies field with one elongated facies. Figure 1b shows one example of the facies field, and, in which, the white shade denotes the facies medium and the black shade denotes the normal reservoir medium. The proportion of the facies medium is 17 %. The permeability and porosity of the facies medium are 1,000 mD and 35 %, respectively. The permeability and porosity of the normal reservoir medium are 50 mD and 15 %, respectively. The distribution of the facies medium is the unknown field. The facies field shown in Fig. 1b is selected as the reference field, which is generated by the SISIM program of the GSLIB Fortran library. The prior geological knowledge is about the facies elongated direction and the directional facies mean lengths. The facies elongated direction is about 30° with the positive x direction, and the directional facies mean lengths in the major and minor correlation directions are approximately 1,000 and

120 ft, respectively. From the reference field, we can see that the facies occurrence near I3 has large lengths in both correlation directions, and the facies occurrence near I1 has small length in the minor correlation direction. The prior information is rough.

In order to perform the history matching, we first design the geostatistical properties of the Gaussian field for parameterizing the facies distribution. Following the discussion at the end of Section 2, the mean and the variance of the Gaussian random field are set to be 0.0 and 0.5, respectively. We select the separable exponential model as the covariance model. The anisotropy direction of the Gaussian field is set to be the same as the anisotropy direction of the facies (i.e., also the facies elongated direction). The correlation lengths in the major and minor correlation directions are set to be equal to the directional facies mean lengths that are 1,000 and 120 ft, respectively. Using Eq. 10, we calculate the level set constant, a, which equals 0.675. The KL expansion is used to parameterize the Gaussian field, and the number of retained terms in the major and minor correlation directions is 10 and 100, respectively.

The model parameter takes the same form as that in Eq. 11, with $n_f = 1$ and $N_1 = 1,000$. The initial realizations of the facies field are generated by sampling of $\{\xi_i\}_{i=1}^{N}$ in the KL expansion and performing the level set algorithm described in Eq. 9. Figure 8a–c shows three initial realizations of the facies field. From these figures, we can see that the generated initial realizations have the same characteristics as the reference; however, the spatial distributions of the initial realizations are different from the reference. Then, we perform the EnRML algorithm to update those global model parameters, and the updated global model parameters are used to construct the new facies field. For EnRML, I_{MAX} is set to be 2. Figure 8d–f shows three updated realizations of the facies field. By comparing these figures with Fig. 1b, we can see that the updated realizations can capture the features of the reference field well and that the geostatistical characteristics of the facies field are preserved in the

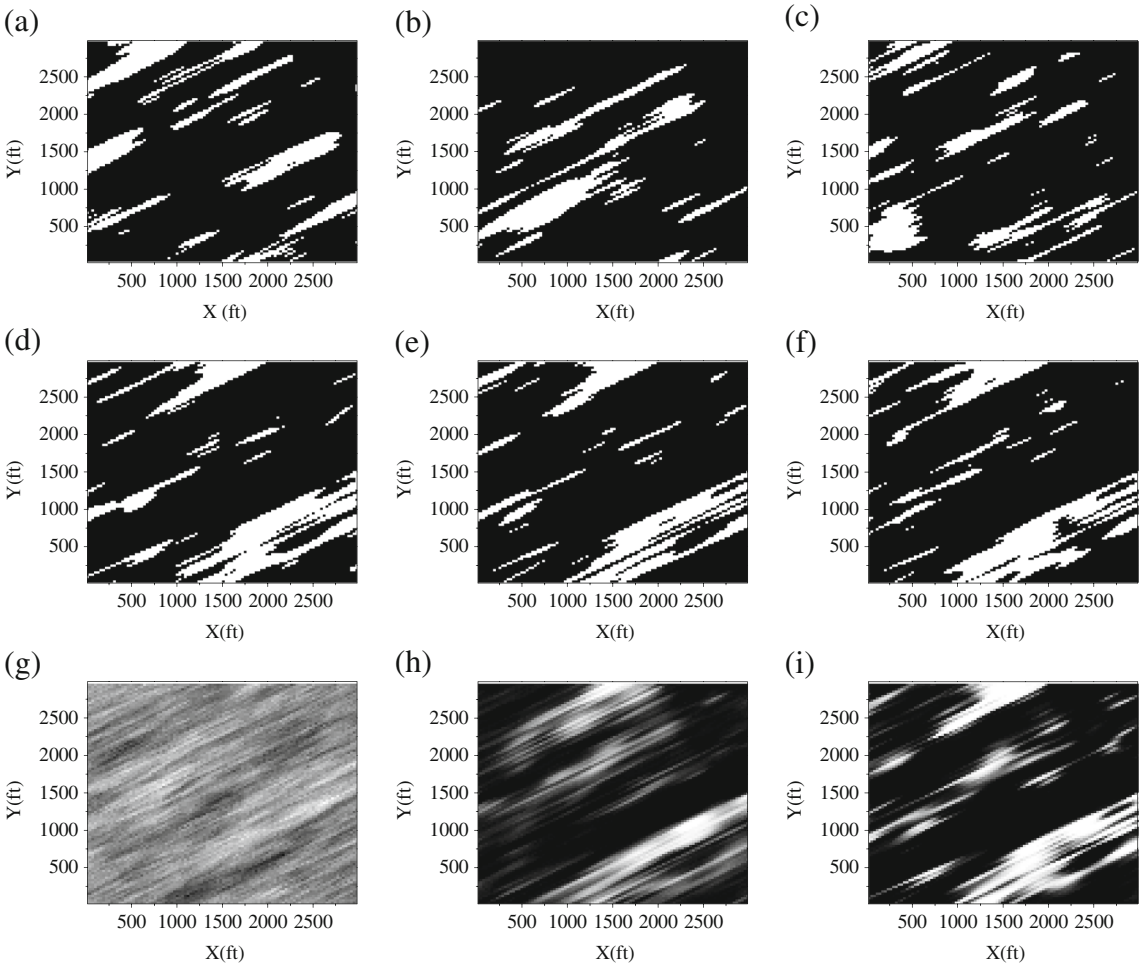

Fig. 8 Three initial realizations of the facies field (**a**–**c**), the corresponding updated realizations (**d**–**f**), and the probabilistic maps from the initial ensemble (**g**), the updated ensemble at step 3 (**h**), and the updated ensemble at step 17 (**i**)

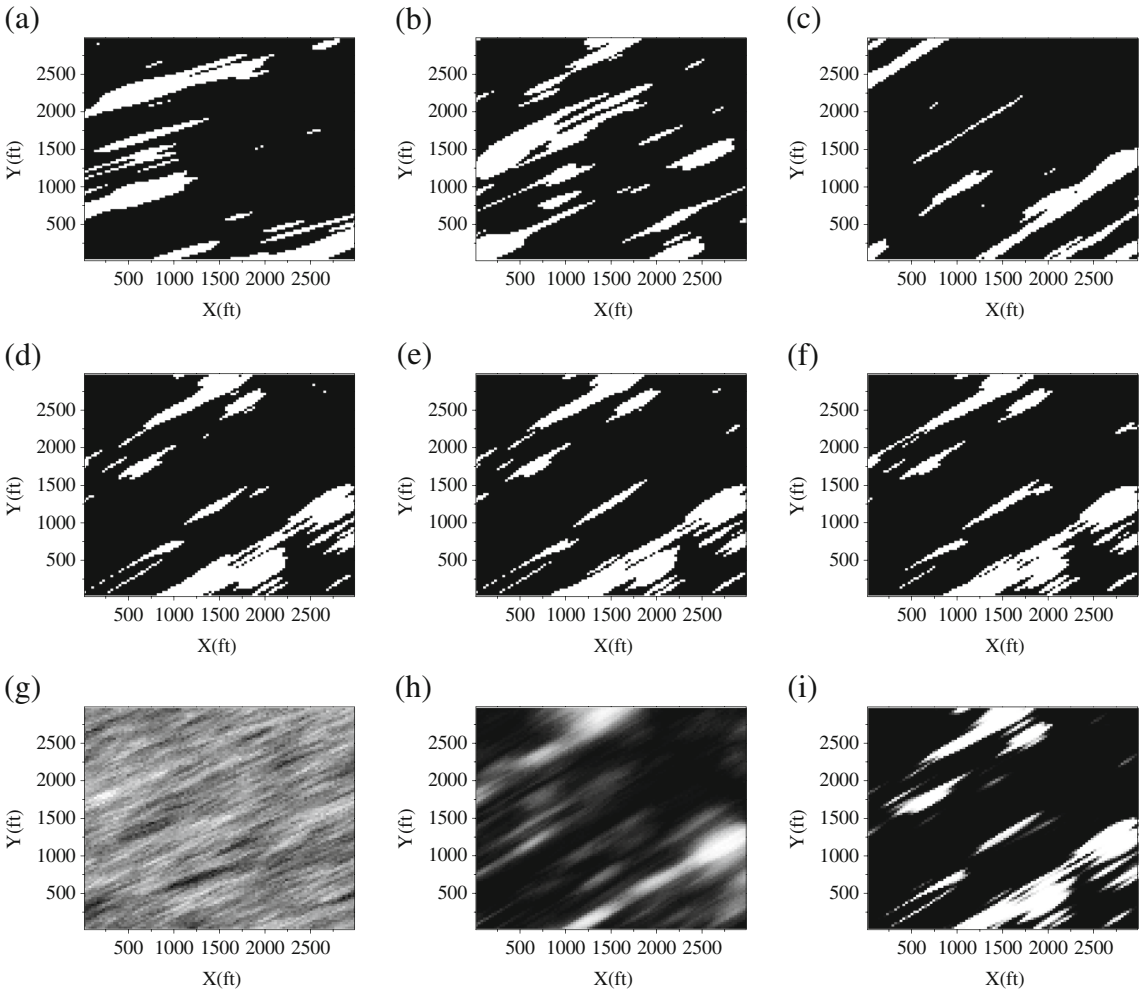

Fig. 9 Three initial realizations of the facies field with uncertain anisotropy direction (**a–c**), the corresponding updated realizations (**d–f**), and the probabilistic maps from the initial ensemble (**g**), the updated ensemble at step 3 (**h**), and the updated ensemble at step 17 (**i**)

updating process. Figure 8g–i shows the probabilistic maps of facies from the initial ensemble and the updated ensemble at step 3 and step 17, respectively. In these maps, the white shade corresponds to a probability of 1, and the black shade corresponds to 0 probability that facies is observed at a specific location in the domain. The different shades of gray represent probability values between 0 and 1. We can see that the probabilistic map from the initial ensemble show approximately equal probability in the whole domain. The probabilistic map from the updated ensemble at step 3 shows some high-probability regions that facies occurrences may occur, and it can approximately indicate the locations

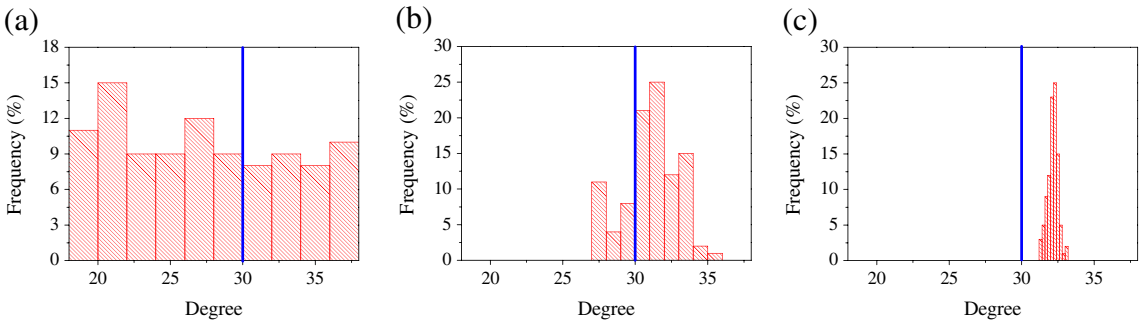

Fig. 10 Histogram of the anisotropy direction of facies from the initial ensemble (**a**), the updated ensemble at step 3 (**b**), and the updated ensemble at step 10 (**c**). The *blue vertical line* indicates the reference value

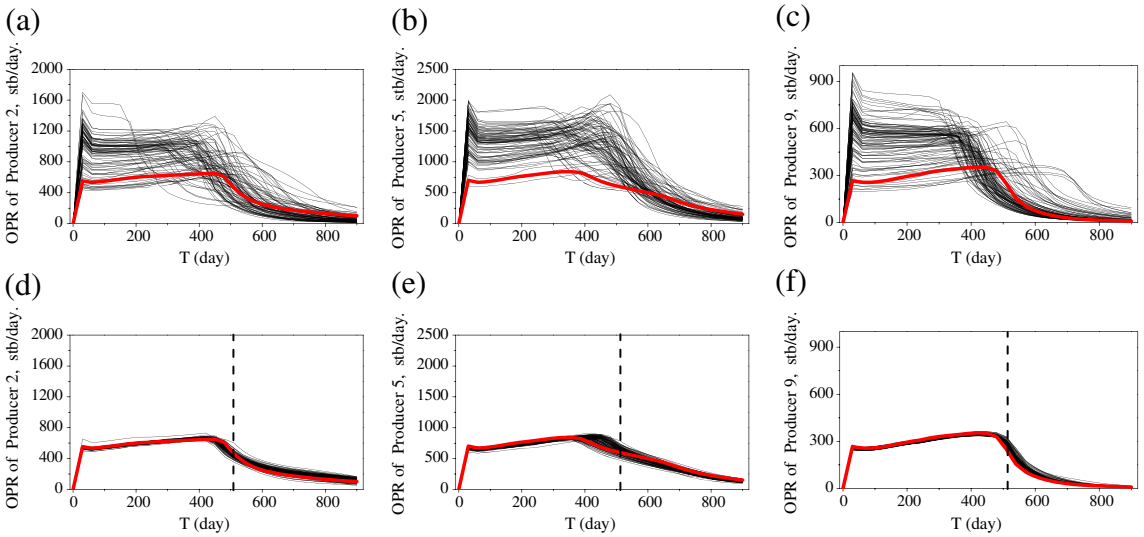

Fig. 11 The match to the oil production rates and the forecast of three producers from the initial ensemble (**a–c**) and the updated ensemble (**d–f**)

of the facies occurrences near I1 and I3 in the reference field. The probabilistic map from the updated ensemble at step 17 can capture the reference facies distribution well, and it also reflects the convergence of the ensemble. In this case, we do not use the facies type measurements at the well locations; if this kind of data is available, a conditional Gaussian random field should be used to parameterize the facies distribution. The Gaussian random variables at the well locations should be set a value that matches the facies types after the level set parameterization. Furthermore the conditional KL expansion can be used to parameterize the conditional Gaussian field and perform the proposed algorithm.

When the anisotropy direction of facies, θ, is uncertain, we treat it as a model parameter. At this time, the model parameter takes the same form as that in Eq. 12, with $n_f = 1$ and $N_1 = 1,000$. In addition to the independent Gaussian random variables, the model parameters contain the anisotropy direction of facies. Here, note that the anisotropy direction of facies is the same as the anisotropy direction of the Gaussian field that is used for parameterizing the facies distribution. For the reference field, θ equals 30°, and this is the reference value. For the initial ensemble, we assume that θ follows $U[18, 38]$. The ensemble of the Gaussian field is generated by sampling of $\{\xi_i\}_{i=1}^{N}$ in the KL expansion and θ in the same way as that described in case 1. Furthermore, the level set algorithm is performed on the Gaussian field ensemble to obtain the initial ensemble of the facies field. Figure 9a–c shows three initial realizations of the facies field. From these figures, we can see that the generated initial realizations have different anisotropy directions of facies. We then perform the EnRML algorithm, and I_{MAX} is set to be 4. Figure 9d–f shows three updated realizations of the facies field. By comparing these figures with Fig. 1b, we can see that the updated realizations can capture the features of the reference field well.

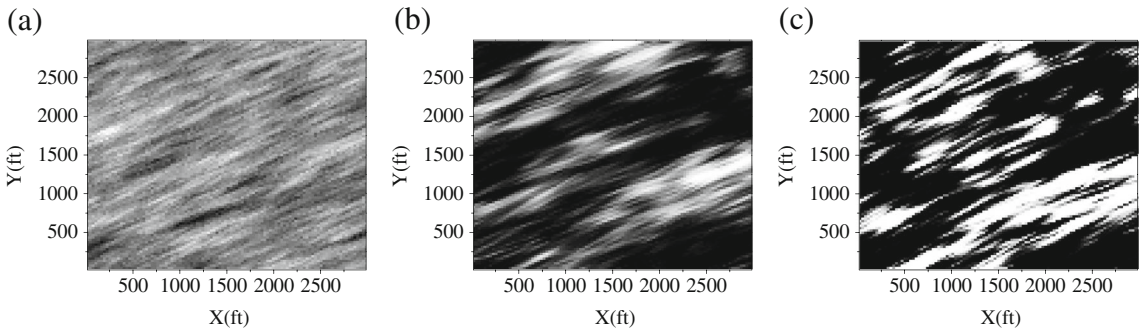

Fig. 12 The probabilistic maps from the initial ensemble (**a**), the updated ensemble at step 3 (**b**), and the updated ensemble at step 17 (**c**) of the facies field with uncertain anisotropy direction using the grid-based parameterization in the history matching method

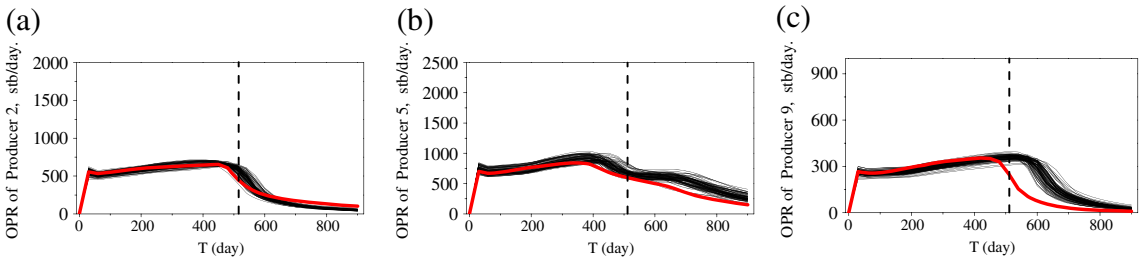

Fig. 13 The match to the oil production rates and the forecast of three producers from the updated ensemble (**a–c**) of the facies field with uncertain anisotropy direction using the grid-based parameterization in the history matching method

Figure 9g–i shows the probabilistic maps of facies from the initial ensemble and the updated ensemble at step 3 and step 17, respectively. We can see that the probabilistic map from the final updated ensemble can capture the reference field well, and the ensemble has good convergence. Figure 10 shows the histogram of the anisotropy direction of facies from the initial ensemble and the updated ensemble at step 3 and step 10. We can see that the updated ensemble at step 3 shows a tendency to converge to the reference value, and that the updated ensemble at step 10 has a mean value 32.4, which is close to but different from the reference value. Figure 11 shows the match to the oil production rates and the forecast of three producers from the initial ensemble (Fig. 11a–c) and the updated ensemble (Fig. 11d–f); we can see that the production behavior from the updated ensemble can match the reference well and can provide a reliable forecast. From Figs. 10 and 11, we can see that although the updated ensemble of the anisotropy direction does not cover the reference, the observation data can be perfectly matched. So the difference between the true anisotropy direction and the updated ensemble cannot be distinguished by the data assimilation process. This slightly biased estimation of the anisotropy direction is reasonable, but it clearly indicates that the uncertainty quantification for anisotropy direction is not enough. To get a better uncertainty quantification for the anisotropy direction, a larger ensemble should be used.

In order to test the necessity of the KL expansion-based parameterization technique used for estimating the elongated facies field with uncertain anisotropy direction and preserving the geostatistical characteristics, we add one more case. In this case, the initial Gaussian field realizations used for parameterizing the facies distribution with uncertain anisotropy direction as shown in Fig. 9a–c are updated using a grid-based parameterization, i.e., the values of the Gaussian field at all the numerical grids are the model parameters and are updated at the data assimilation steps. The updated Gaussian field realizations are used to obtain the facies distribution realizations using Eq. 9. Figure 12a–c shows the probabilistic maps of facies from the initial ensemble and the updated ensemble at step 3 and step 17, respectively. From these probabilistic maps, we can see that the updated ensemble can approximately estimate the locations of the reference facies occurrences, but it indicates some wrong facies occurrences. The anisotropy direction of the reference field is not captured well by the updated ensemble, and this may be caused by the differences of the anisotropy direction in the initial Gaussian field realizations and the grid-based local parameterization. Figure 13 shows the match to the oil production rates and the forecast of three producers from the updated ensemble. We can see that the forecasts for producer 2 and producer 5 are slightly biased, and the forecast for producer 9 is largely biased.

By comparing the above cases, we can see that the KL expansion-based global parameterization is more appropriate than the grid-based local parameterization for estimating the elongated facies distribution with uncertain anisotropy direction.

4.3 Case 3: facies field with two elongated facies

In this subsection, we discuss the history matching of the facies field with two elongated facies. Figure 1c shows one example of the facies field, in which the white shade denotes facies 1, the black shade denotes facies 2, and the gray shade denotes the normal reservoir medium. Facies 1 and facies 2 have equal proportions, which is 14 %. The permeability of facies 1, facies 2, and the normal reservoir medium are 1,000, 0.1, and 50 md, respectively. The porosity of facies 1, facies 2, and the normal medium are 35, 10, and 20 %, respectively. Facies 1 acts as a high-permeability channel, and facies 2 acts as a low-permeability barrier. The distributions of the two facies are the unknown fields. The facies field shown in Fig. 1c is selected as the reference field. This reference field is generated by the level set algorithm described in Eq. 9 using two Gaussian random fields respectively, and an assumption that facies 1 will occupy the locations passed by both facies 1 and facies 2. The assumption used will not affect the result much by considering that the intersection area of the two facies in the reference field

is not large. When dealing with the field that the intersection area of different facies is large, a parameterization of the formation sequence should be taken. The two Gaussian random fields for generating the reference field are generated by KL expansion with truncated terms.

In this case, the geostatistical properties of the Gaussian fields for parameterizing the two facies distributions are known. So, there is no prior error about the geostatistical properties of the Gaussian fields for parameterization. The mean and the variance of the two Gaussian random fields are 0.0 and 0.5, respectively. The covariance model is separable exponential model. The anisotropy directions of the two Gaussian fields are the same as the anisotropy directions of the two facies, respectively. The correlation lengths in the major and minor correlation directions are 1,500 and 150 ft, respectively. The level set constant equals 0.76. The

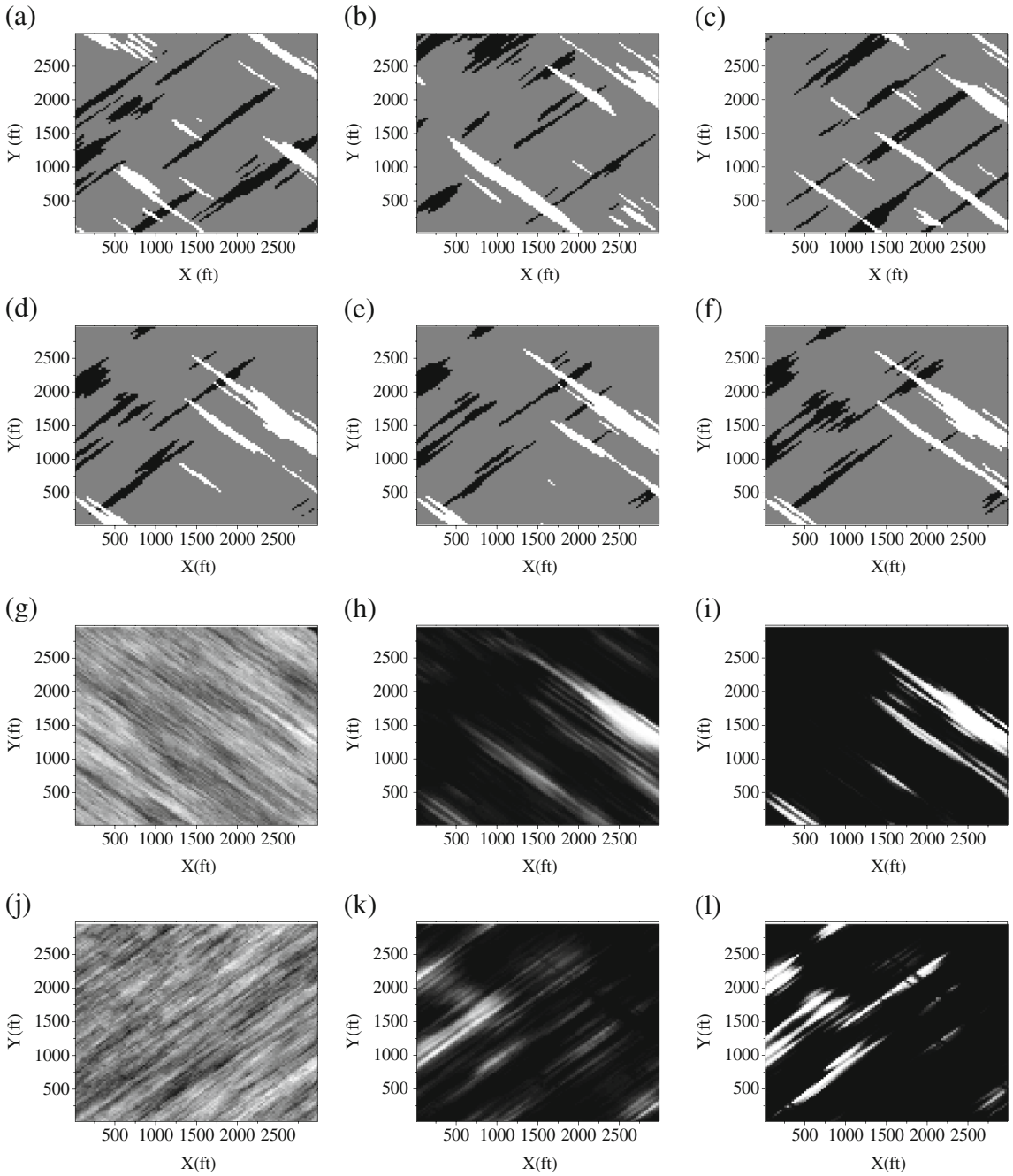

Fig. 14 Three initial realizations of the facies field (**a**–**c**), the corresponding updated realizations (**d**–**f**), and the probabilistic maps for facies 1 and facies 2 from the initial ensemble (**g**, **j**), the updated ensemble at step 3 (**h**, **k**), and the updated ensemble at step 17 (**i**, **l**)

KL expansion is used to parameterize the Gaussian fields, and the number of retained terms in the major and minor correlation directions is 8 and 80, respectively.

The model parameter takes the same form as that in Eq. 11, with $n_f = 2$ and $N_1 = N_2 = 640$. The initial realizations of the facies field are generated by sampling two groups of independent Gaussian random variables and performing the level set algorithm. Figure 14a–c shows three initial realizations of the facies field. We then perform the EnRML algorithm, and I_{MAX} is set to be 2. Figure 14d–f shows three updated realizations of the facies field. By comparing these figures with Fig. 1c, we can see that the updated realizations can capture the features of the reference field well. Figure 14g–i shows the probabilistic maps of facies 1

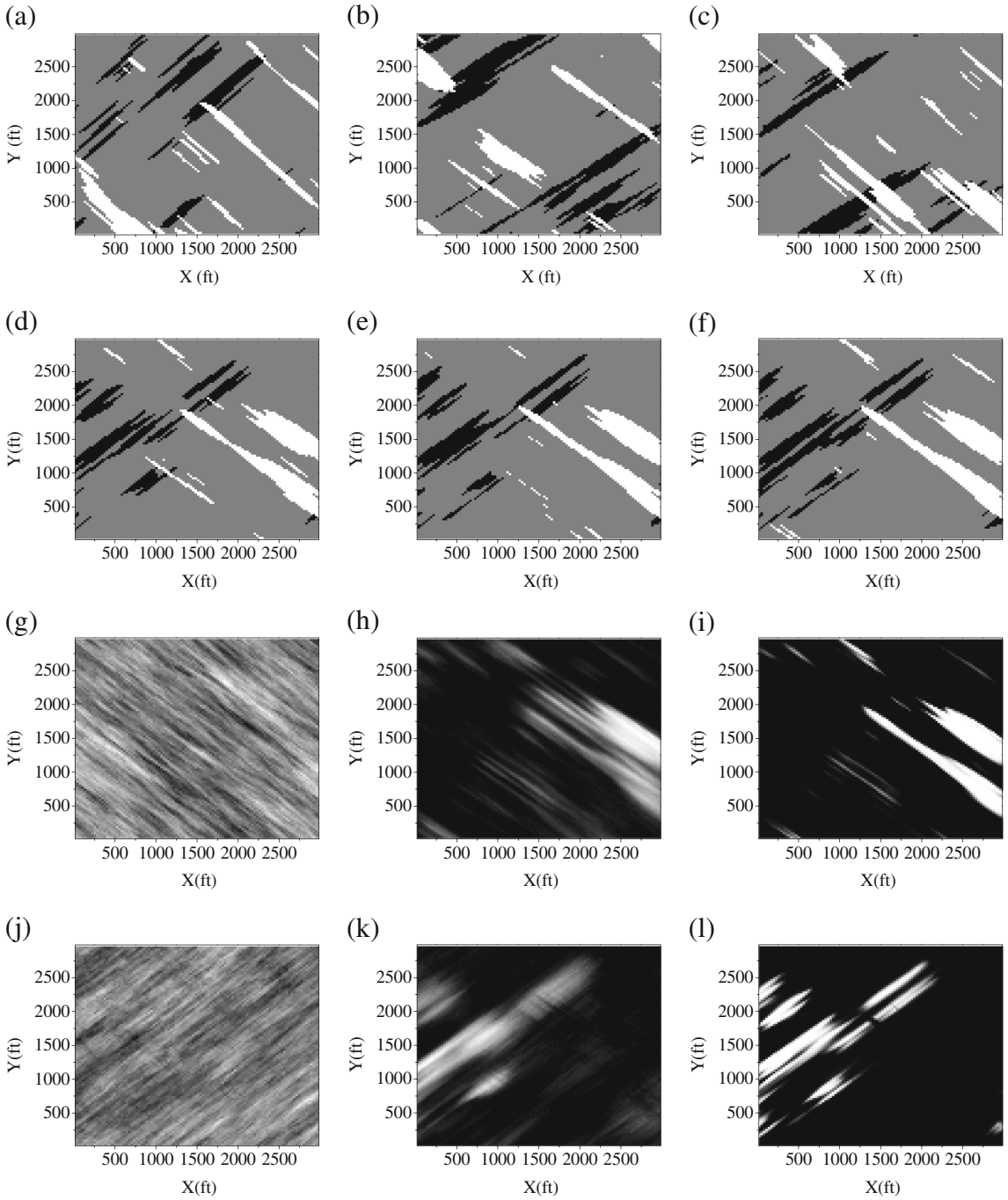

Fig. 15 Three initial realizations of the facies field with uncertain anisotropy directions (**a**–**c**), the corresponding updated realizations (**d**–**f**), and the probabilistic maps for facies 1 and facies 2 from the initial ensemble (**g**, **j**), the updated ensemble at step 3 (**h**, **k**), and the updated ensemble at step 17 (**i**, **l**)

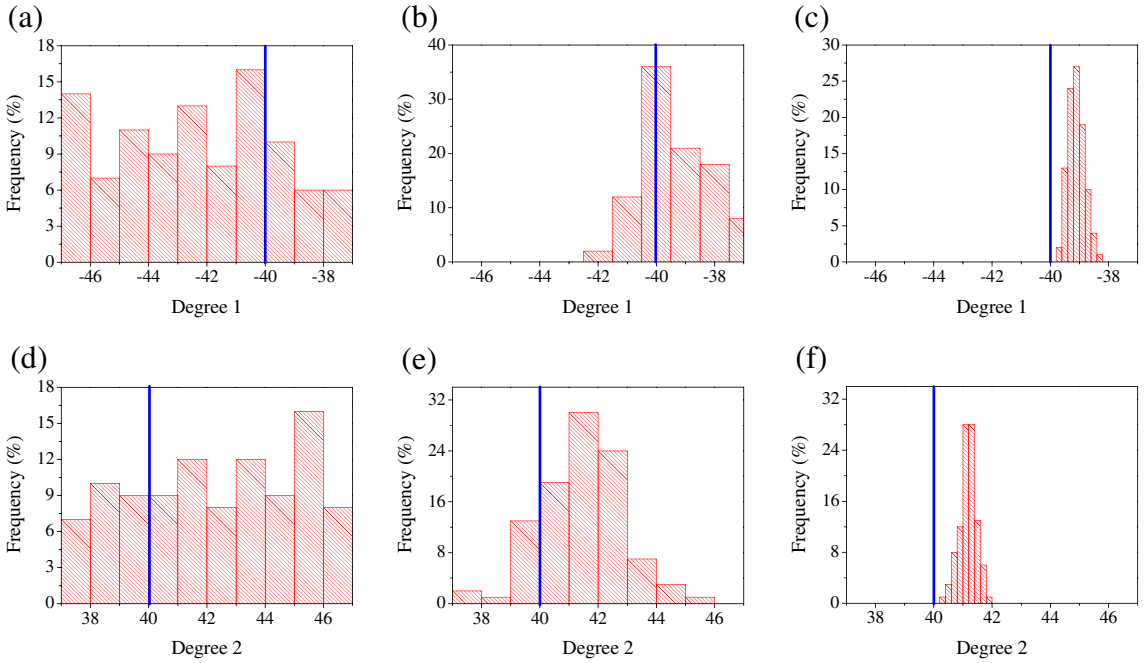

Fig. 16 Histogram of the anisotropy direction of facies 1 (**a**–**c**) and the anisotropy direction of facies 2 (**d**–**f**) from the initial ensemble (**a**, **d**), the updated ensemble at step 3 (**b**, **e**), and the updated ensemble at step 15 (**c**, **f**). The *blue vertical line* indicates the reference value

from the initial ensemble and the updated ensemble at step 3 and step 17, respectively. Figure 14j–l shows the probabilistic maps of facies 2 from the initial ensemble and the updated ensemble at step 3 and step 17, respectively. From the probabilistic maps, we can see that updated ensemble at step 17 has a good convergence and can estimate the facies distributions well.

When the anisotropy directions of facies are uncertain, we treat them as model parameters. At this time, the model parameter takes the same form as that in Eq. 12, with $n_f = 2$ and $N_1 = N_2 = 640$. For the reference field, the anisotropy direction of facies 1, θ_1, equals $-40°$, and the anisotropy direction of facies 2, θ_2, equals 40°. For the initial ensemble, we assume that θ_1 follows U[-47, -37], and θ_2 follows U[37, 47]. Figure 15a–c shows three initial realizations of the facies field. From these figures, we can see that the generated initial realizations have different anisotropy directions of facies. We then perform the EnRML algorithm,

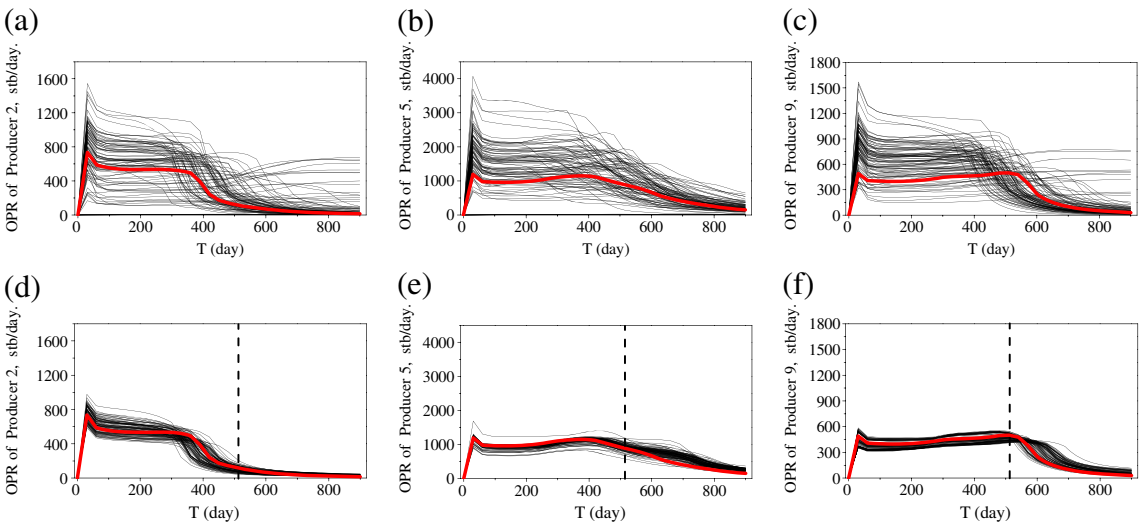

Fig. 17 The match to the oil production rates and the forecast of three producers from the initial ensemble (**a**–**c**) and the updated ensemble (**d**–**f**)

and I_{MAX} is set to be 4. Figure 15d–f shows three updated realizations of the facies field. Figure 15g–l shows the probabilistic maps of the two facies from the initial ensemble and the updated ensemble at step 3 and step 17. From the updated realizations and the updated probabilistic maps, we can see that the updated results can capture the main features of the reference well. Figure 16 shows the histogram of the anisotropy directions of the two facies from the initial ensemble and the updated ensemble at step 3 and step 15. We can see that the updated ensembles at step 3 show a tendency to converge to the reference values and that the updated ensemble of θ_1 and θ_2 at step 15 has mean value of 39.1° and 41.2°, respectively, which are close to the reference values. Figure 17 shows the match to the oil production rates and the forecast of three producers from the initial ensemble (Fig. 17a–c) and the updated ensemble (Fig. 17d–f); we can see that the production behavior from the updated ensemble can match the reference well and can provide reliable forecast.

5 Discussion and conclusion

In the history matching process, the parameter field will be continuously updated. Using a numerical grid-based local parameterization technique makes it difficult to preserve the geostatistical characteristics of the parameter fields. The KL expansion is a proper global parameterization technique to preserve the geostatistical characteristics of a Gaussian parameter field in the updating process of the history matching method. In this work, we propose a KL expansion-based global parameterization technique for the history matching of statistically anisotropic fields. For a Gaussian field or facies field with a known correlation structure, by using the KL expansion, it can be parameterized by a group of independent Gaussian random variables, which can be treated as model parameters. When the anisotropy direction of the unknown random field is uncertain, it can also be treated as a model parameter for updating. We adopt the EnRML algorithm to perform the history matching. Three kinds of parameter fields (i.e., a statistically anisotropic Gaussian field, a facies field with one elongated facies, and a facies field with two elongated facies) are selected as the reference parameter fields to test the performance of the proposed method. The case studies show that, by using the KL expansion-based global parameterization technique, the updated results can match the reference well and the geostatistical characteristics of the random field can be preserved in the updating process. Using the proposed method, the estimation of the anisotropy direction of the random field is satisfactory.

One drawback of the global parameterization technique is that it is difficult to capture all the local features of the unknown field. If the data matches in some regions of the reservoir are not satisfactory, using some local parameters in those regions to refine the parameterization is a way to solve the problem.

The KL expansion-based global parameterization technique is only suitable for parameterizing Gaussian random fields (that can be completely depicted by the first two moments). For non-Gaussian random fields, such as curvilinear channels or fractures, other parameterization techniques should be investigated.

In this work, although we only use two-dimensional cases to test the proposed method, the KL expansion-based method can be easily extended to three-dimensional problems.

Acknowledgments This work is partially funded by the National Science and Technology Major Project of China through grants 2011ZX05009-006 and 2011ZX05052, the National Key Technology R&D Program of China (Grant No. 2012BAC24B02), the Public Project of the Ministry of Land and Resources of China (Grant No. 201211063), the China Postdoctoral Science Foundation (Grant No. 2012M510276), and the National Natural Science Foundation of China (Grant No. 51304008).

References

1. Aanonsen, S.I., Naevdal, G., Oliver, D.S., Reynolds, A.C., Valles, B.: The ensemble Kalman filter in reservoir engineering—a review. SPE J. **14**(3), 393–412 (2009)
2. Agbalaka, C.C., Oliver, D.S.: Application of the EnKF and localization to automatic history matching of facies distribution and production data. Math. Geosci. **40**(4), 353–374 (2008)
3. Caers, J.: Efficient gradual deformation using a streamline-based proxy method. J. Pet. Sci. Eng. **39**, 57–83 (2003a)
4. Caers, J.: History matching under training-image-based geological model constraints. SPE J. **7**, 218–226 (2003b)
5. Caers, J., Hoffman, T.: The probability perturbation method: a new look at Bayesian inverse modeling. Math. Geol. **38**(1), 81–100 (2006)
6. Chang, H., Zhang, D., Lu, Z.: History matching of facies distribution with the EnKF and level set parameterization. J. Comput. Phys. **229**, 8011–8030 (2010)
7. Evensen, G., Hove, J., Meisingset, H.C., Reiso, E., Seim, K.S., Espelid, O.: Using the EnKF for assisted history matching of a North Sea reservoir model. In: Proceedings of SPE Reservoir Simulation Symposium, Houston, 26–28 February (2007)
8. Galli A., Beucher, H., Le Loc'h, G., Doligez, B., Group, H.: The pros and cons of the truncated Gaussian method. In: Geostatistical Simulations, pp. 217–233. Kluwer Academic, Dordrecht (1994)
9. Ghanem, R., Spanos, P.: Stochastic Finite Element: A Spectral Approach. Springer, New York (1991)
10. Gu, Y., Oliver, D.S.: An iterative ensemble Kalman filter for multiphase fluid flow data assimilation. SPE J. **12**(4), 438–446 (2007)
11. Hoffman, B.T., Caers, J.: Regional probability perturbations for history matching. J. Pet. Sci. Eng. **46**, 53–71 (2005)

12. Hu, L.Y.: Gradual deformation and iterative calibration of Gaussian-related stochastic models. Math. Geol. **32**(1), 87–108 (2000)
13. Hu, L.Y.: Extended probability perturbation method for calibration stochastic reservoir models. Math Geosci. **40**, 875–885 (2008)
14. Hu, L.Y., Blanc, G., Noetinger, B.: Gradual deformation and iterative calibration of sequential stochastic simulations. Math. Geol. **33**, 475–489 (2001)
15. Jafarpour, B., McLaughlin, D.B.: History matching with an ensemble Kalman filter and discrete cosine parameterization. Comput. Geosci. **12**(2), 227–244 (2008)
16. Karhunen, K.: Uber lineare Methoden in der Wahrscheinlichkeitsrechnung. Ann. Acad. Sci. Fen. Ser. A. I. Math. Phys. **37**, 1–79 (1947)
17. Le Loc'h, G., Galli, A.: Truncated plurigaussian method: theoretical and practical points of view. In: Baafi, E.Y., Schofiled, N.A (eds.) Geostatistics Wollongong '96, vol. 1, pp. 211–222. Kluwer Academic (1997)
18. Li, G., Reynolds, A.C.: An iterative ensemble Kalman filter for data assimilation. In: Proceedings of SPE Annual Technical Conference and Exhibition, Anaheim, California, 11–14 November (2007)
19. Li, H., Zhang, D.: Probabilistic collocation method for flow in porous media: comparisons with other stochastic methods. Water Resour. Res. (2007). doi:10.1029/2006WR005673
20. Liu, N., Oliver, D.S.: Ensemble Kalman filter for automatic history matching of geologic facies. J. Pet. Sci. Eng. **47**(3-4), 147–161 (2005)
21. Loeve, M.: Fonctions aleatoires de second order. In: Levy P (ed) Processus Stochastiques et Movement Brownien. Hermann, Paris (1948)
22. Lu, Z., Zhang, D.: Conditional simulations of flow in randomly heterogeneous porous media using a KL-based moment-equation approach. Adv. Water Resour. **27**, 859–871 (2004)
23. Naevdal, G., Mannseth, T., Vefring, E.H.: Near-well reservoir monitoring through ensemble Kalman filter. In: Proceedings of SPE/DOE Improved Oil Recovery Symposium, Tulsa, Oklahoma, 13–17 April (2002)
24. Naevdal, G., Johnsen, L.M., Aanonsen, S.I., Vefring, E.H.: Reservoir monitoring and continuous model updating using ensemble Kalman filter. SPE J. **10**(1), 66–74 (2005)
25. Reynolds, A.C., He, N., Chu, L., Oliver, D.S.: Reparameterization techniques for generating reservoir descriptions conditioned to variograms and well-test pressure data. SPE J. **1**, 413–426 (1996)
26. Roggero, F., Hu, L.Y.: Gradual deformation of continuous geostatistical models for history matching. In: Proceedings of SPE Annual Technical Conference and Exhibition, New Orleans, Louisiana, 27–30 September (1998)
27. Romary, T.: Integrating production data under uncertainty by parallel interacting Markov chains on a reduced dimensional space. Comput. Geosci. **13**(1), 103–122 (2009)
28. Sarma, P., Durlofshy, L.J., Aziz, K., Chen, W.H.: Efficient real-time reservoir management using adjoint-based optimal control and model updating. Comput. Geosci. **10**(1), 3–36 (2006)
29. Thulin, K., Li, G., Aanonsen, S.I., Reynolds, A.C.: Estimation of initial fluid contacts by assimilation of production data with EnKF. In: Proceedings of SPE Annual Technical Conference and Exhibition, Anaheim, California, 11–14 November (2007)
30. Zafari, M., Li, G., Reynolds, A.C.: Iterative forms of the ensemble Kalman filter. In: Proceedings of the 10th European Conference on the Mathematics of Oil Recovery, Amsterdam, p. A030 (2006)
31. Zeng, L., Chang, H., Zhang, D.: A probabilistic collocation-based Kalman filter for history matching. SPE J **16**(2), 294–306 (2010)
32. Zhang, D., Lu, Z.: An efficient, high-order perturbation approach for flow in random porous media via Karhunen-Loeve and polynomial expansions. J. Comput. Phys. **194**, 773–794 (2004)
33. Zhang, D., Lu, Z., Chen, Y.: Dynamic reservoir data assimilation with an efficient, dimension-reduced Kalman filter. SPE J. **12**(1), 108–117 (2007)